

Angle-Resolved Photoemission Spectroscopy of the Insulating Na_xWO_3 : Anderson Localization, Polaron Formation, and Remnant Fermi Surface

S. Raj,^{1,*} D. Hashimoto,¹ H. Matsui,¹ S. Souma,¹ T. Sato,^{1,2} T. Takahashi,^{1,2} D. D. Sarma,^{3,†} Priya Mahadevan,⁴ and S. Oishi⁵

¹*Department of Physics, Tohoku University, Sendai 980-8578, Japan*

²*CREST, Japan Science and Technology Agency (JST), Kawaguchi 332-0012, Japan*

³*Solid State and Structural Chemistry Unit, Indian Institute of Science, Bangalore 560 012, India*

⁴*S. N. Bose National Centre for Basic Sciences, JD Block, Sector 3, Salt Lake, Kolkata 700 098, India*

⁵*Faculty of Engineering, Shinshu University, Nagano 380-8553, Japan*

(Received 18 October 2005; published 12 April 2006)

The electronic structure of the insulating sodium tungsten bronze, $\text{Na}_{0.025}\text{WO}_3$, is investigated by high-resolution angle-resolved photoemission spectroscopy. We find that near- E_F states are localized due to the strong disorder arising from random distribution of Na^+ ions in the WO_3 lattice, which makes the system insulating. The temperature dependence of photoemission spectra provides direct evidence for polaron formation. The remnant Fermi surface of the insulator is found to be the replica of the real Fermi surface in the metallic system.

DOI: [10.1103/PhysRevLett.96.147603](https://doi.org/10.1103/PhysRevLett.96.147603)

PACS numbers: 79.60.-i, 71.18.+y, 71.30.+h

The physical properties of materials are strongly influenced by electronic interactions and randomness [1]. In particular, electron correlations and disorder are the main driving forces behind metal-insulator transitions (MITs) associated with the localization and delocalization of particles. The disorder driven MIT, which is known as an Anderson-type transition, arises from the localization of states near the Fermi level (E_F) due to strong disorder created by randomly distributed impurities [2]. The localized charge carriers could induce a lattice distortion resulting in the formation of a polaron and get trapped even further. Polaron signatures are currently discussed in many compounds such as colossal magnetoresistance manganites [3], charge ordered nickelates, and bismuthates [4]. The simultaneous effect of disorder and polaron formation have not been well understood. In this work we consider the example of lightly doped Na_xWO_3 ($x = 0.025$) and show from high-resolution angle-resolved photoemission studies that disorder leads to a soft Coulomb gap opening up in this system. We have chosen low x value in Na_xWO_3 to reduce the disorder and inelastic scattering of electrons and as an effect we see sharper peaks leading to clear band dispersion. Simultaneously, in another energy window, we find evidence suggestive of a polaron formation which shows strong temperature dependence of spectral features. Examining the band dispersions as a function of temperature, one finds the polaronic feature becomes more delocalized as the temperature is increased. To our knowledge this is the first time that disorder effects as well as polaron formation have been studied in the same system. The present study provides valuable inputs for constructing effective models for the electronic structure of this class of materials where disorder effects and polaron effects are simultaneously present.

Na_xWO_3 exhibits a rich phase diagram with both structural transitions as well as metal-insulator transitions taking place as a function of x (Ref. [5]). The origin of the metal-insulator transition is still under debate as electron correlations, disorder as well as impurity band formation, have been cited as possible causes [6–11]. In this work we show that the variation of the density of states near E_F is suggestive of an Anderson-type localization of carriers for the ground state. The most interesting aspect of these results is that the remnant Fermi surface (FS) left behind as a result of carrier localization is very similar to the real Fermi surface of the metallic system after taking into account the surface reconstruction which is an output of our low energy electron diffraction (LEED) studies.

Single crystals of $\text{Na}_{0.025}\text{WO}_3$ were grown from a high-temperature solution of $\text{Na}_2\text{O}-\text{WO}_3$ by a slow cooling method [12]. ARPES measurements were performed using a GAMMADATA-SCIENTA SES-200 spectrometer with a high-flux discharge lamp. The He I α ($h\nu = 21.218$ eV) resonance line was used to excite photoelectrons. The energy and angular (momentum) resolutions were set at 5–11 meV and 0.2° (0.01 \AA^{-1}), respectively. A clean surface of sample for photoemission measurements was obtained by *in situ* cleaving along (001) surface. The possibility of charging in the insulating sample was checked by reducing the photon flux. We found no shift in the valence-band peaks, which confirms that there is no charging in the sample. The Fermi level of the sample was referred to that of a gold film evaporated on the sample substrate and its accuracy was estimated to be better than 1 meV.

Figure 1 shows the valence-band ARPES spectra of $\text{Na}_{0.025}\text{WO}_3$ measured at 130 K along $\Gamma(X)-X(M)$ and $\Gamma(X)-M(R)$ directions in the Brillouin zone (BZ). In $\text{Na}_{0.025}\text{WO}_3$, E_F is situated in the conduction band and

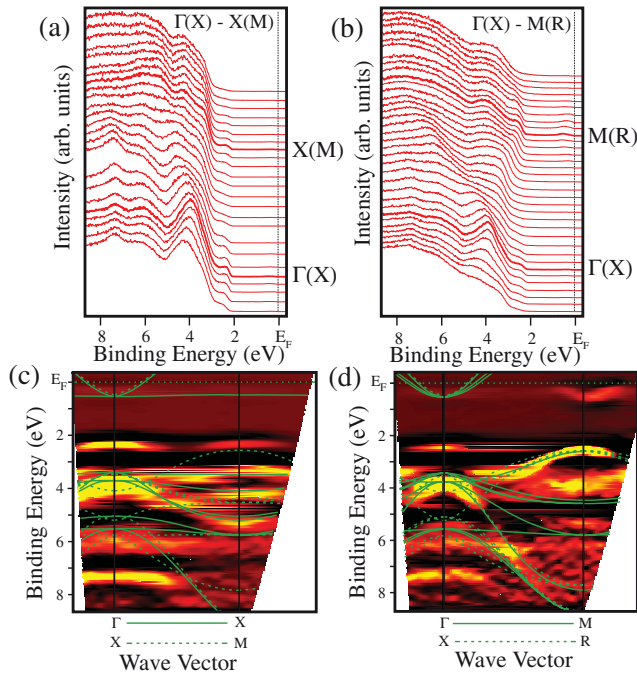


FIG. 1 (color). Valence-band ARPES spectra of $\text{Na}_{0.025}\text{WO}_3$ measured along (a) $\Gamma(X)$ - $X(M)$ and (b) $\Gamma(X)$ - $M(R)$ in BZ at 130 K. Experimental valence-band structure along (c) $\Gamma(X)$ - $X(M)$ and (d) $\Gamma(X)$ - $M(R)$ obtained from ARPES experiments. Yellow bright areas correspond to the experimental bands. The theoretical band structure of WO_3 after shifting E_F is also shown by thin solid and dashed lines for comparison.

the bottom of conduction band lies at 0.5 eV binding energy as clearly visible around $M(R)$ point. The top of the valence band extends up to 2.5 eV binding energy. The most prominent peak in the valence band is seen at 4.0 eV along with two other broad peaks at 6.0 and 7.3 eV around $\Gamma(X)$, which disperse downward by going toward zone boundaries. We also show in Fig. 1 the experimental band structure of $\text{Na}_{0.025}\text{WO}_3$. The experimental band structure has been obtained by taking the second derivative of the ARPES spectra. The pseudopotential band structure using projected augmented wave potential [13–15] of cubic WO_3 is also shown for comparison. Within a rigid-band model, the band structure of both WO_3 and NaWO_3 should be identical with E_F at different positions. The calculated Fermi level shifts 2.2 eV upward as we move from WO_3 to NaWO_3 (Ref. [16]). In Figs. 1(c) and 1(d), we shift the calculated E_F of WO_3 by about 1.15 eV upward to overlap with experimental bands. The top of the valence band at 2.5 eV and the band at 7.4 eV around $\Gamma(X)$ are not predicted in the band calculation. The band around 4.0 eV at $\Gamma(X)$, which disperses highly along both $\Gamma(X)$ - $X(M)$ and $\Gamma(X)$ - $M(R)$ directions is in good agreement with the band calculation. The valence band consists of mostly the O $2p$ states of $\text{Na}_{0.025}\text{WO}_3$ with a small admixture of bonding W $5d$ states.

To see more clearly the conduction band, we measured ARPES spectra in the near- E_F region at 130 K and the

results are shown in Fig. 2. We observe a peak near 0.45 eV at $\Gamma(X)$, which disperses upward around $\Gamma(X)$. A similar feature is observed around both $X(M)$ and $M(R)$ points. This dispersive peak represents the conduction band of $\text{Na}_{0.025}\text{WO}_3$, which never cross E_F , showing that the system is insulating. Figs. 2(c) and 2(d) show the plot of ARPES intensity at near- E_F region. We find an electron-like pocket at $\Gamma(X)$, whose dispersion agrees satisfactorily with the band calculation. The conduction band is assigned as the W $5d t_{2g}$ orbital from the band calculation. A similar electronlike pocket is also observed at $X(M)$ and $M(R)$ points, contrary to the band calculation. This may be due to the surface reconstruction, which we discuss later. The insulating behavior arises from the Anderson localization of all the states near E_F due to the strong disorder caused by inserting Na in a WO_3 lattice. Simultaneously a soft Coulomb gap arises at E_F and consequently the density of states (DOS) vanishes at E_F . This gap arises due to the long-range interaction of the electrons trapped due to the strong disorder caused by Na doping. We fit the experimental DOS (not shown) near E_F with a function of $(E - E_F)^\alpha + C$, where C is a constant, and found that α is close to 2. Hence, we conclude that the presence of disorder together with long-range Coulomb interactions leads to the formation of a soft Coulomb gap at E_F in this system, this being responsible for its insulating properties. The possibility of splitting of the band due to electron correlation at the chemical potential (or E_F) into two bands, originally proposed by Mott [7], is unlikely in case of $\text{Na}_{0.025}\text{WO}_3$. Such correlation-driven gaps at the E_F can form only if the band has integral occupancy. This is obviously not the case for any arbitrary value of x in general; specifically, the occupancy of W $5d$ is only a

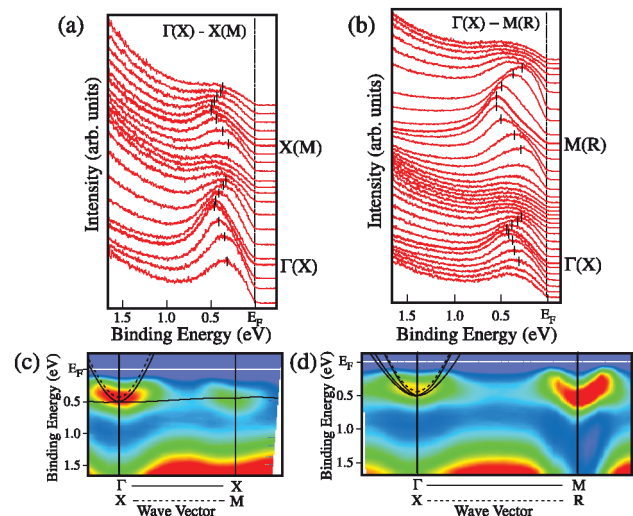


FIG. 2 (color). ARPES spectra near E_F of $\text{Na}_{0.025}\text{WO}_3$ measured along (a) $\Gamma(X)$ - $X(M)$ and (b) $\Gamma(X)$ - $M(R)$ in BZ at 130 K. Vertical bars are a guide to eyes for band dispersion. Experimental near- E_F band structure along (c) $\Gamma(X)$ - $X(M)$ and (d) $\Gamma(X)$ - $M(R)$. Theoretical band structure of WO_3 after shifting E_F is also shown by thin solid and dashed lines for comparison.

fractional 0.025 per site in the compound investigated here. Moreover, the Coulomb repulsion (U) is expected to be weak and the tungsten $5d$ band width (W) large in $\text{Na}_{0.025}\text{WO}_3$ to satisfy Mott-Hubbard criterion of $U/W \gg 1$. On the other hand, the low DOS at band bottom for the small x value favors localization of states due to disorder effects. The possibility of a weak localization [17] without any Coulomb gap formation is unlikely in the present case, since there has been no evidence of an insulator-to-metal-like change in the conductivity of these compounds with increasing temperature. Reich and Tsabba [18] reported surface superconductivity with T_c as high as 91 K in the lightly doped sodium tungsten bronzes, $\text{Na}_{0.05}\text{WO}_3$. Our data near E_F does not support this idea. We did not observe any finite DOS at E_F above T_c for $x = 0.025$ with our high-resolution measurements [Figs. 2(a) and 2(b)]. Hence we conclude that there is no such superconductivity on the surface of the lightly doped sodium tungsten bronzes.

Figure 3 shows valence-band photoemission spectroscopy (PES) spectra of $\text{Na}_{0.025}\text{WO}_3$ at $\Gamma(X)$ (within 14° acceptance angle of detector) with variation of temperature. All the spectra are normalized under the curve within the range shown in Fig. 3. We clearly see the variation of intensity of the 2.5 eV peak with temperature. Band structure calculation does not predict the existence of a 2.5 eV peak at $\Gamma(X)$ point and our PES spectra see mostly the angle-integrated spectra around $\Gamma(X)$. Benbow and Hurych [8] explained this peak as due to the plasmon excitation. However, plasmon excitation is unlikely in the insulating system. To explore whether this feature corresponds to the surface states or not, we carry out PES with He II α ($h\nu = 40.8$ eV) photons, which is much more surface sensitive than He I α photons. We do not see any reasonable DOS at

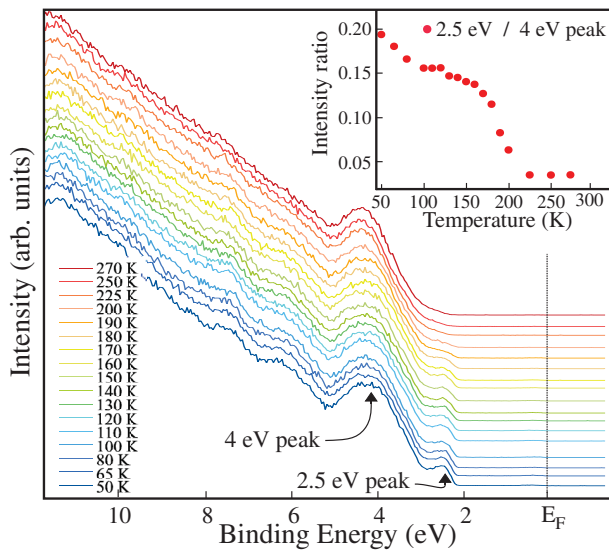


FIG. 3 (color). Valence-band PES spectra of $\text{Na}_{0.025}\text{WO}_3$ at several temperatures showing the signature of polaron formation at valence-band edge, 2.5 eV. The inset shows the temperature dependence of the intensity ratio of the 2.5 eV peak to the 4.0 eV peak.

2.5 eV due to the 3-dimensional band structure of this band implying its bulk origin. The reproducibility of the intensity variation of 2.5 eV peak with temperature cycling was also established. It is believed that at low sodium doping levels, the sodium tungsten bronzes are nonmetallic with localized W^{5+} and W^{6+} ions and show polaronic states [19,20]. Polarons can form in the insulating system, particularly when the conduction electrons are in a comparatively narrow d band and are contributed by donors distributed at random in the lattice. The polaron formation in the lightly doped tungsten bronzes were studied with electron spin resonance, optical absorption, and Raman spectroscopy [19,21]. The conduction electrons are self-trapped by inducing an asymmetric local deformation of the lattice. Even if the electron is confined to a single lattice site, this type of trapping does not imply localization. The tunneling between different lattice sites is still relevant and a self-trapped carrier resides in an itinerant polaron state [22]. This is most likely to occur when the band edge is degenerate and the valence-band edge is more often degenerate than the conduction band edge, so that holes are more likely to be self-trapped than electrons. We think that the change in the intensity of 2.5 eV peak is due to the breakdown of polaron formation at higher temperatures (above 225 K). In the inset of Fig. 3, we show the intensity ratio of valence-band edge (2.5 eV peak) to 4 eV peak. We find that the intensity of 2.5 eV peak decreases with increasing temperature and reaches minimum above 225 K. Above this temperature, the holes or electrons are no longer self-trapped. Polaron can be considered as a local deformations or defects in the lattice and a truly localized defect level is derived primarily from the Γ point ($k = 0$) with far less weight from other k points. A more delocalized defect level is derived from k points other than Γ [23]. The temperature dependence of the polaronic features is the first time observation of the dynamics of the polaron. As the polaron becomes more delocalized, there is spectral weight transfer from Γ to other k points. In Fig. 3 we mainly observe the intensity around Γ point and as a result the intensity decreases with increasing temperature. The optical absorption of W^{5+} in WO_3 shows the signature of polaron formation in low temperature and vanishes at 300 K (Ref. [19]). Hence we conclude that the increase in intensity of valence-band edge below 225 K is likely due to the formation of polaron. The polaron can split or broaden the edge of valence band but due to the temperature-induced broadening in the spectra, we did not find any significant splitting or broadening of the band edge with temperature.

In Fig. 4(a), we show the ARPES-intensity plot at E_F as a function of a two-dimensional wave vector. The intensity is obtained by integrating the spectral weight within 80 meV with respect to E_F and symmetrized on assuming the cubic symmetry. The conduction band arising from the $\text{W } 5d t_{2g}$ orbital disperses upward [Figs. 2(a) and 2(b)] but never crosses E_F . Our finding reveals a remnant Fermi

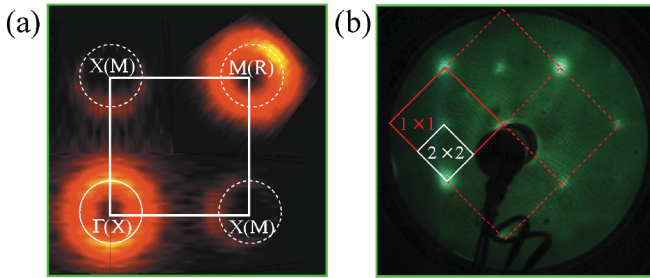


FIG. 4 (color). (a) Remnant Fermi surfaces of $\text{Na}_{0.025}\text{WO}_3$ at 130 K in the first Brillouin zone. Solid and dashed circles show the highest intensity points. (b) LEED pattern of (001) cleaved surface measured with primary energy of 54 eV at 130 K. It shows the 1×1 bulk and the 2×2 surface superlattice spots.

surface even though $\text{Na}_{0.025}\text{WO}_3$ shows insulating behavior due to Anderson localization. A similar remnant Fermi surface is observed in other insulator, $\text{Ca}_2\text{CuO}_2\text{Cl}_2$ (Ref. [24]). From the high quality data near E_F we establish that the remnant Fermi surface observed at $\Gamma(X)$ in this insulating phase has a shape similar to the real Fermi surface in metallic sodium tungsten bronzes which one expect in the absence of any disorder in metallic phase and matches well to the band calculation. We find similar Fermi surfaces at $X(M)$ and $M(R)$ and we infer that this is due to the surface reconstruction. We carried out the LEED for the (001) cleaved surface with primary energy of 54 eV at 130 K and the result is shown in Fig. 4(b). In the LEED pattern, we see the 1×1 bulk and the 2×2 surface superlattice spots. The 2×2 superlattice spots regenerate the $X(M)$ and $M(R)$ points as a new $\Gamma(X)$ point in ARPES. Hence, the surface reconstruction is confirmed from our LEED measurement. Now, we discuss in more detail the surface reconstruction, which may create two-dimensional electronic states on the first few layers different from the bulk states. Such surface-reconstruction-derived bands were found in the ARPES spectra of Sr_2RuO_4 (Ref. [25]). The rotation and deformation of the WO_6 octahedra in $\text{Na}_{0.025}\text{WO}_3$ give rise to the orthorhombic crystal structure. In the bulk, the rotation is small and we think that the rotation of the WO_6 octahedra increases at the surface due to the reduced atomic coordination, which is responsible for the surface reconstruction in $\text{Na}_{0.025}\text{WO}_3$ as similarly observed in Sr_2RuO_4 (Ref. [25]). In Fig. 2(b), we see that the band bottom at $M(R)$ is different from $\Gamma(X)$, which imply that the surface bands interact with the bulk bands and the surface bands at $M(R)$ are not completely two-dimensional. We observe that the intensity at $M(R)$ point is stronger than other points probably due to the matrix element effects.

In conclusion, we have directly observed the band dispersion and the remnant Fermi surface of $\text{Na}_{0.025}\text{WO}_3$ by high-resolution ARPES. We concluded that the near- E_F states are localized due to the strong disorder arising from the random distribution of Na^+ ions in WO_3 lattice, which makes the system insulating. Because of the disorder and

long-range Coulomb interactions, a soft Coulomb gap arises and the density of states vanishes at E_F . We found direct evidence of polaron formation from the temperature dependence of the photoemission spectra. We found that the remnant FS is the replica of the real FS observed in the metallic system.

This work is supported by grants from JST-CREST, JSPS and MEXT of Japan. S.R. thanks the 21st century COE program ‘‘Exploring new science by bridging particle-matter hierarchy’’ for financial support. H.M. and S.S. acknowledge the financial support from JSPS.

*Electronic address: raj@arpes.phys.tohoku.ac.jp

†Also at Jawaharlal Nehru Centre for Advanced Scientific Research, Bangalore 560 054, India.

- [1] A. Lee and T. V. Ramakrishnan, *Rev. Mod. Phys.* **57**, 287 (1985); D. Belitz and T.R. Kirkpatrick, *Rev. Mod. Phys.* **66**, 261 (1994).
- [2] P. W. Anderson, *Phys. Rev.* **109**, 1492 (1958).
- [3] A. J. Millis, *Nature (London)* **392**, 147 (1998).
- [4] E. K. H. Salje *et al.*, *Polarons and Bipolarons in High Temperature Superconductors and Related Materials* (Cambridge University Press, Cambridge, 1995).
- [5] H. R. Shanks, P. H. Slides, and G. C. Danielson, *Non Stoichiometric Compounds*, *Advance in Chemistry Series Vol. 39* (American Chemical Society, Washington, DC, 1963) p. 237; A. S. Ribnick, B. Post, and E. Banks, *ibid.* Vol. 39 p. 246 (1963).
- [6] N. F. Mott, *Proc. Phys. Soc. London, Sect. A* **62**, 416 (1949).
- [7] N. F. Mott, *Philos. Mag.* **35**, 111 (1977).
- [8] R. L. Benbow and Z. Hurych, *Phys. Rev. B* **17**, 4527 (1978).
- [9] M. D. Hill and R. G. Egdell, *J. Phys. C* **16**, 6205 (1983).
- [10] G. Hollinger *et al.*, *Phys. Rev. B* **32**, 1987 (1985).
- [11] E. Sonder and N. K. Stevens, *Phys. Rev.* **110**, 1027 (1958).
- [12] S. Oishi, N. Endo, and K. Kitajima, *Nippon Kagaku Kaishi* (The Chemical Society of Japan, Japan, 1995), Vol. 11, p. 891.
- [13] P. E. Blöchl, *Phys. Rev. B* **50**, 17 953 (1994).
- [14] G. Kresse and D. Joubert, *Phys. Rev. B* **59**, 1758 (1999).
- [15] G. Kresse and J. Furthmüller, *Phys. Rev. B* **54**, 11 169 (1996); *Comput. Mater. Sci.* **6**, 15 (1996).
- [16] S. Raj *et al.*, *Phys. Rev. B* **72**, 125125 (2005).
- [17] G. Bergmann, *Phys. Rev. B* **28**, 2914 (1983); *Phys. Rep.* **107**, 1 (1984).
- [18] S. Reich and Y. Tsabba, *Eur. Phys. J. B* **9**, 1 (1999).
- [19] O. F. Schirmer and E. Salje, *Solid State Commun.* **33**, 333 (1980); *J. Phys. C* **13**, L1067 (1980).
- [20] E. Salje and B. Guttler, *Philos. Mag. B* **50**, 607 (1984).
- [21] R. G. Egdell and G. B. Jones, *J. Solid State Chem.* **81**, 137 (1989).
- [22] H. DeRaedt and A. Lagendijk, *Phys. Rev. B* **27**, 6097 (1983); H. Lowen, *ibid.* **37**, 8661 (1988); J. Ranninger and U. Thibblin, *ibid.* **45**, 7730 (1992).
- [23] G. F. Koster and J. C. Slater, *Phys. Rev.* **95**, 1167 (1954).
- [24] F. Ronning *et al.*, *Science* **282**, 2067 (1998).
- [25] R. Matzdorf *et al.*, *Science* **289**, 746 (2000).